Stars as Suns: Activity, Evolution, and Planets
IAU Symposium, Vol. 219, 2004
A. K. Dupree and A. O. Benz, Eds.

The Structure and Dynamics of the Outer Atmosphere of ϵ Eri

S. A. Sim

Astrophysics Group, Imperial College London, Blackett Laboratory, Prince Consort Road, London, SW7 2BW, UK

C. Jordan

Department of Physics (Theoretical Physics), University of Oxford, 1 Keble Road, Oxford, OX1 3NP, UK

Abstract. We present results from our study of the active dwarf ϵ Eri (K2 V) based on ultraviolet spectra recorded with the Space Telescope Imaging Spectrograph and the Far Ultraviolet Spectroscopic Explorer. A combination of simple theoretical arguments and observational constraints derived from measured line fluxes are used to deduce new information about the structure of the upper transition region/corona. The area filling factor of emitting material is determined in the upper atmosphere as a function of temperature. This provides new constraints on how the magnetic field might spread out in the atmosphere of an active main sequence star. Measured emission line widths are used, together with a new semi-empirical model of the atmosphere, to place limits on the energy fluxes carried by MHD waves. These are compared with estimates of the energy input required to support the combined radiative/conductive losses in the upper atmosphere. It is shown that, in principle, waves which propagate at the Alfvén speed could provide sufficient energy to heat the corona.

1. Introduction

We briefly discuss two aspects of our recent study of the active dwarf star ϵ Eri: first we present results relating to the area filling factor of emitting material in the upper atmosphere and secondly on the possibility of coronal heating by waves. These results, and the Space Telescope Imaging Spectrograph (STIS) and Far Ultraviolet Spectroscopic Explorer (FUSE) data used to derive them, are discussed more fully by Sim & Jordan (2003a,b).

2. Area filling factors

In this section, we show how the area filling factor of emitting material $A(r)/A_*(r)$ in the upper atmosphere can be obtained by comparing observed and theoretical emission measure distributions. ($A(r)$ is the surface area at radius r occupied by emitting material and $A_*(r) = 4\pi r^2$ is the total surface area.) We work in terms

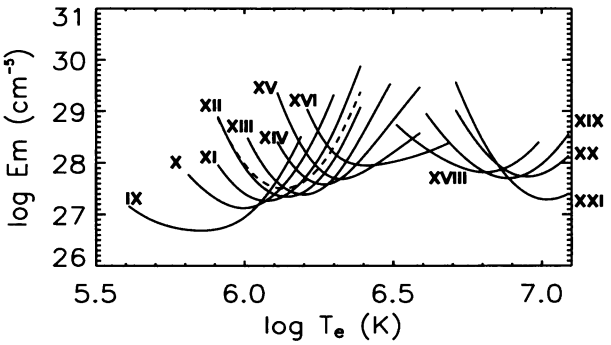

Figure 1. Apparent emission measure loci. The solid curves were computed using the iron line fluxes reported by Schmitt et al. (1996) (labelled with the ionization stage they represent). The dashed curve was obtained using the Fe XII 1242-Å flux from Jordan et al. (2001).

of the apparent mean emission measure distribution (EMD) which we denote $Em^{0.3}$ (see Sim & Jordan 2003a for our formal definition of this quantity).

2.1. Constraints from observations

The EMD can be constrained by measurements of emission line fluxes (see e.g. Jordan & Brown 1981). For ϵ Eri, we have used iron line fluxes reported by Schmitt et al. (1996) to construct loci which constrain the EMD in the upper transition region/inner corona (see Sim & Jordan 2003a). Figure 1 shows these upper bounds (solid curves) together with an additional constraint derived from the Fe XII line flux measured with STIS (Jordan et al. 2001, dashed curve). These loci suggest that the EMD increases smoothly through the upper transition region to a peak at several million degrees Kelvin. Above this temperature the EMD drops. At temperatures significantly above the peak, most of the emission probably originates in active regions.

The greatest source of error in the derived emission measure loci is the adopted ionization balance. The loci shown in Figure 1 were computed with the ionization calculations of Arnaud & Raymond (1992). However, calculations have also been performed using the Arnaud & Rothenflug (1985) ionization balance which are significantly different for several of the ions considered here (in particular Fe IX, XV and XVI – see Sim & Jordan 2003a).

2.2. Theoretical EMD

Jordan (2000) has shown how the form of the EMD in the upper transition region can be determined theoretically based on an energy balance between radiation and conduction. The theory predicts $Em^{0.3}A_*(r)/A(r)$ as a function of temperature (see Sim & Jordan 2003a): a typical computed EMD is shown in Figure 2.

2.3. Area filling factors

By combining the observational constraints (§ 2.1) and a theoretical model (§ 2.2), the area filling factor of emitting material ($A(r)/A_*(r)$) may be esti-

https://doi.org/10.1017/S0074180900182208 Published online by Cambridge University Press

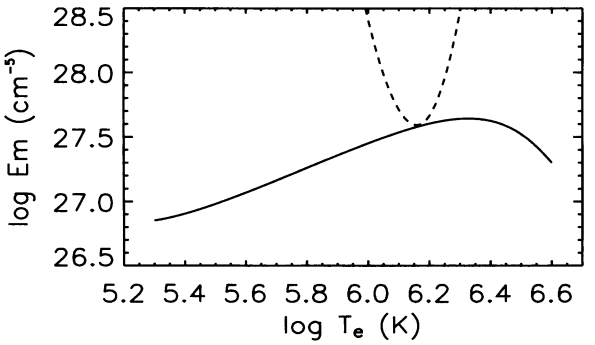

Figure 2. Theoretical $Em^{0.3}A_*(r)/A(r)$ curve (solid line). The dashed line is the STIS Fe XII locus from Figure 1 for comparison.

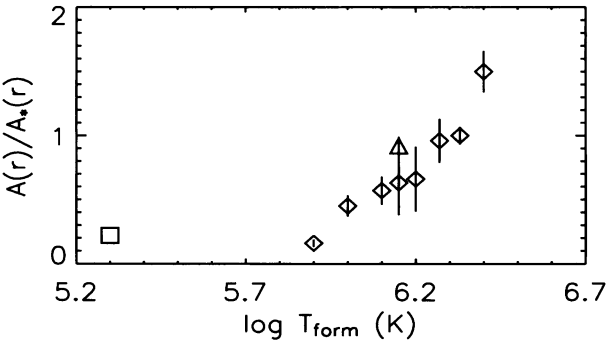

Figure 3. Area filling factor as a function of temperature in ϵ Eri. The diamonds indicate results based on the iron line fluxes reported by Schmitt et al. (1996), the triangle shows that using the Fe XII flux from Jordan et al. (2001) and the box is based on comparison with a mid-transition region EMD determined from STIS line fluxes (Sim 2002). The error bars only indicate measurement errors in the line fluxes, not systematic errors (see text).

mated. The area factors deduced in this way are plotted in Figure 3. The results are subject to several systematic errors (discussed by Sim & Jordan 2003a) which mean that area factors derived from individual lines may be in error by up to a factor of 2 – 3. This explains the unphysical $A(r)/A_*(r)$ value for Fe XVI (the highest temperature point in Figure 3). However, for most of the lines the systematic errors are much smaller ($\sim$ several tens per cent).

The results indicate that $A(r)/A_*(r)$ increases from $\sim$20 per cent in the mid-transition region to $\sim$100 per cent in the corona. This behaviour is broadly similar to that found from observations of the Sun (Gallagher et al. 1998) and the Gabriel (1976) transition region model. In future work, this method will be applied to other stars to investigate trends in the filling factor with stellar activity, and a wider range of observed line fluxes will be utilized to eliminate sources of systematic error.

https://doi.org/10.1017/S0074180900182208 Published online by Cambridge University Press

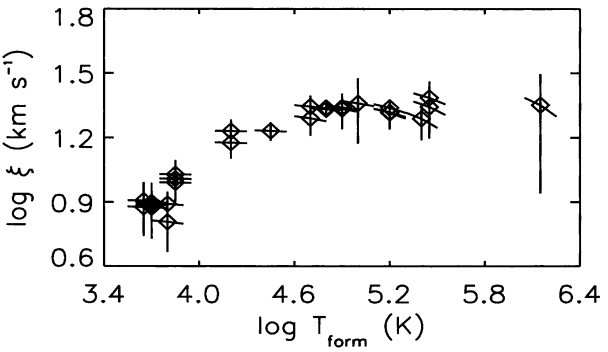

Figure 4. Most probable non-thermal velocity versus temperature for ϵ Eri.

3. Wave heating

In this section we use line width measurements to constrain the amount of energy that could be supplied by waves for coronal heating.

3.1. Observed non-thermal line widths

We have measured line widths for a wide range of emission lines from STIS and FUSE spectra of ϵ Eri and used these to deduce the most probable non-thermal velocity (ξ, see Sim & Jordan 2003b). Figure 4 shows ξ versus the temperature of line formation and indicates that the non-thermal velocity varies smoothly, increasing from about 8 km s^{-1} in the chromosphere to $\sim$21 km s^{-1} in the upper transition region. This is qualitatively similar to equivalent results for the Sun (see e.g. Chae, Schühle, & Lemaire 1998).

3.2. Energy fluxes

As discussed by Sim & Jordan (2003b), the non-thermal line widths may be combined with an atmospheric model (Sim 2002) to place an upper limit on the spatially averaged non-thermal energy flux ($F_{\rm NT}A(r)/A_*(r)$) by assuming that the non-thermal motions are caused by passing MHD waves. This limit can then be compared to the energy requirements of the corona to test the possibility of heating by wave dissipation.

Figure 5 shows the non-thermal energy flux versus temperature for waves that propagate at the Alfvén speed. In the chromosphere $T_{\rm form} < 10^4$ K two sets of results are plotted: one in which perfect coupling between neutrals and ions is assumed (filled symbols) and the other where no coupling occurs (open symbols). With perfect coupling, the chromospheric radiation losses far exceed those observed. Above 10^4 K the neutral component is negligible. The calculations assume that all the surface magnetic flux (determined by Rüedi et al. 1997) extends to the corona. If only a fraction b of the surface flux extends to a given height, then the energy flux at that height would be reduced by the factor b. The solid line shows the flux required at every point to support the radiation losses above that point (computed from the atmospheric model).

https://doi.org/10.1017/S0074180900182208 Published online by Cambridge University Press

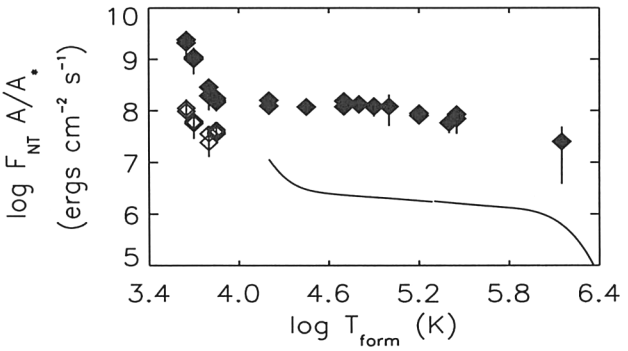

Figure 5. The solid and open diamonds indicate upper limits on the non-thermal energy flux that could be carried by waves which propagate at the Alfvén speed for two different cases (see text). The solid line shows the flux required to supply radiation losses.

The results indicate that MHD waves could carry sufficient energy to support the heating requirements of the corona, even if b is only $\sim$0.1 in the corona. The apparent drop in the energy flux between $\log T_{\rm form}({\rm K}) = 5.6$ and 6.1 presents a challenge to the wave heating theory: the drop is too large to be explained by local dissipation (it cannot be the result of varying b since b can only decrease with temperature). However, this apparent decrease could be the result of complex wave reflection/transmission in the transition region which is not taken into account here (see Sim & Jordan 2003b for discussion).

References

Arnaud, M., & Raymond, J. 1992, ApJ, 398, 394

Arnaud, M., & Rothenflug, R. 1985, A&AS, 60, 425

Chae, J., Schühle, U., & Lemaire, P. 1998, ApJ, 505, 957

Gabriel, A. H. 1976, Phil. Trans. Roy. Soc. London, A281, 339

Gallagher, P. T., Phillips, K. J. H., Harra-Murnion, L. K., & Keenan, F. P. 1998, A&A, 335, 733

Jordan, C. 2000, Plasma Phys. Control. Fusion, 42, 415

Jordan, C., & Brown, A., 1981, in NATO ASIC, 68, Solar Phenomena in Stars and Stellar Systems, ed. R. M. Bonnet & A. K. Dupree (Reidel. Dordrecht, Holland), 199

Jordan, C., McMurry, A. D., Sim, S. A., & Arulvel M. 2001, MNRAS, 322, L5

Rüedi, I., Solanki, S. K., Mathys, G., & Saar, S. H. 1997, A&A, 318, 429

Schmitt, J. H. M. M., Drake, J. J., Stern, R. A., & Haisch, B. M. 1996, ApJ, 457, 882

Sim, S. A. 2002, D.Phil Thesis, University of Oxford

Sim, S. A., & Jordan, C. 2003a, MNRAS, 346, 846

Sim, S. A., & Jordan, C. 2003b, MNRAS, 341, 517